ATP-binding Cassette Transporter A1 Mediates the Beneficial Effects of the Liver X Receptor Agonist GW3965 on Object Recognition Memory and Amyloid Burden in Amyloid Precursor Protein/Presenilin 1 Mice*[S]

James J. Donkin[‡1], **Sophie Stukas**[‡2], **Veronica Hirsch-Reinshagen**[‡], **Dhananjay Namjoshi**[‡], **Anna Wilkinson**[‡], **Sharon May**[‡], **Jeniffer Chan**[‡], **Jianjia Fan**[‡], **Jon Collins**[§], and **Cheryl L. Wellington**[‡3]

From the [‡]*Department of Pathology and Laboratory Medicine, Child and Family Research Institute, University of British Columbia, Vancouver, British Columbia V5Z 4H4, Canada and* [§]*Glaxo-Smith Kline, Research Triangle Park, North Carolina 27709*

The cholesterol transporter ATP-binding cassette transporter A1 (*ABCA1*) moves lipids onto apolipoproteins including apolipoprotein E (*apoE*), which is the major cholesterol carrier in the brain and an established genetic risk factor for late-onset Alzheimer disease (AD). In amyloid mouse models of AD, *ABCA1* deficiency exacerbates amyloidogenesis, whereas *ABCA1* overexpression ameliorates amyloid load, suggesting a role for *ABCA1* in Aβ metabolism. Agonists of liver X receptors (LXR), including GW3965, induce transcription of several genes including *ABCA1* and *apoE,* and reduce Aβ levels and improve cognition in AD mice. However, the specific role of *ABCA1* in mediating beneficial responses to LXR agonists in AD mice is unknown. We evaluated behavioral and neuropathical outcomes in GW3965-treated female APP/PS1 mice with and without *ABCA1*. Treatment of APP/PS1 mice with GW3965 increased *ABCA1* and *apoE* protein levels. *ABCA1* was required to observe significantly elevated *apoE* levels in brain tissue and cerebrospinal fluid upon therapeutic (33 mg/kg/day) GW3965 treatment. At 33 mg/kg/day, GW3965 was also associated with a trend toward redistribution of Aβ to the carbonate-soluble pool independent of *ABCA1*. APP/PS1 mice treated with either 2.5 or 33 mg/kg/day of GW3965 showed a clear trend toward reduced amyloid burden in hippocampus and whole brain, whereas APP/PS1-treated mice lacking *ABCA1* failed to display reduced amyloid load in the whole brain and showed trends toward increased hippocampal amyloid. Treatment of APP/PS1 mice with either dose of GW3965 completely restored novel object recognition memory to wild-type levels, which required *ABCA1*. These results suggest that *ABCA1* contributes to several beneficial effects of the LXR agonist GW3965 in APP/PS1 mice.

Lipid metabolism is increasingly recognized to play a key role in the pathogenesis of Alzheimer disease (AD),[4] which is the leading cause of dementia in the elderly (1). AD is characterized by the presence of two neuropathological hallmarks including extracellular amyloid plaques that consist mainly of aggregated Aβ peptides and intracellular neurofibrillary tangles consisting of hyperphosphorylated Tau protein (2). Although the pathogenesis of AD is not completely understood, a leading hypothesis is that aberrant metabolism of Aβ peptides, which are derived by proteolytic cleavage from amyloid precursor protein (APP), triggers many of the toxic events in AD and eventually leads to both Tau and amyloid pathologies (3). Less than 5% of AD patients exhibit disease onset in their 40s and 50s due to genetic mutations that lead to increased production of Aβ peptides, particularly of the most detrimental Aβ42 species (4). The cause of AD in more than 95% of subjects that typically develop AD in late life is unknown. As production of Aβ is generally not altered in these patients, age-related defects in Aβ degradation and clearance is emerging as a leading hypothesis for development of AD in the majority of patients (5).

In mice, *apoE* exists in only one allelic state, whereas humans possess three allelic isoforms: *apoE*2 (Cys^{112} and Cys^{158}), *apoE*3 (Cys^{112} and Arg^{158}), and *apoE*4 (Arg^{112} and Arg^{158}) (14). In 1993, *apoE* genotype was identified as a robust genetic factor for late-onset AD. Specifically, inheritance of *apoE*4 increases the risk and reduces the age of onset of AD (15), whereas *apoE*2 delays onset and reduces risk (16). Precisely how *apoE* functions in AD pathogenesis remains incompletely understood. *ApoE* binds Aβ (17) and affects amyloid load in mice in an isoform-specific manner (18). *ApoE* is the primary lipid transporter in the brain and plays major roles in the repair and regeneration of neuronal membranes (8). Additionally, *apoE* possesses anti-inflammatory activity, and inflammation has a key role in AD pathogenesis (19). Several recent studies have demonstrated that the amount of lipids carried by *apoE* is a critical determinant of Aβ metabolism. Specifically, lipid-enriched *apoE* may facilitate Aβ degradation and clearance (6–14).

---

[4] The abbreviations used are: AD, Alzheimer disease; APP, amyloid precursor protein; PS1, presenilin 1; MWM, Morris water maze; CSF, cerebrospinal fluid; CTF, COOH-terminal fragment; BisTris, 2-[bis(2-hydroxyethyl)amino]-2-(hydroxymethyl)propane-1,3-diol; NOR, novel object recognition; LXR, liver X receptor.

The most cholesterol-rich organ in the body is the brain, which contains ~25% of total body cholesterol in only 2% of total body weight (15). Lipid metabolism in the central nervous system is based entirely upon lipoproteins that resemble plasma high-density lipoproteins (HDL: the "good cholesterol") in density, size, and composition (16). The major difference between brain and plasma HDL is that *apoE* is the predominant protein constituent of brain HDL, whereas *apoA-I* is the predominant protein on plasma HDL (16, 17).

The rate-limiting step in HDL biogenesis is catalyzed by the lipid transporter *ABCA1*, which effluxes cholesterol and phospholipids from the plasma membrane to lipid-free apolipoproteins (18–20). In peripheral tissues, the primary apolipoprotein acceptor for *ABCA1* activity is *apoA-I* (18–20), whereas it is *apoE* in the brain (6, 9). Deficiency of murine *ABCA1* leads to poorly lipidated *apoE* in the central nervous system (6, 9), which facilitates the formation of amyloid deposits in AD mice (7, 8, 11). Conversely, selective overexpression of *ABCA1* by 6-fold or more is sufficient to increase central nervous system *apoE* lipidation and prevent the formation of amyloid plaques in mice (10).

Consistent with the hypothesis that *ABCA1*-mediated lipidation of *apoE* affects Aβ metabolism are the results of genetic and pharmacological manipulation of pathways regulated by α and β liver X receptors (LXRs). LXRα/β are ligand-activated transcription factors of the nuclear hormone receptor superfamily that stimulate transcription of several genes, including *ABCA1* and *apoE* (21, 22). LXRα and LXRβ respond to the same oxysterol ligands and activate transcription as obligate heterodimeric complexes with retinoid X receptors (21, 22). Most LXR target genes, including *ABCA1* and *apoE*, have functions related to cholesterol and lipoprotein metabolism, whereas other LXR target genes act to reduce inflammation (23). Genetic deficiency of either LXRα or LXRβ increases amyloid burden in AD mice (24). Conversely, synthetic LXR agonists, including TO901317 and GW3965, activate both LXRα and LXRβ (25–27), cross the blood-brain barrier, and efficiently induce expression of LXR target genes including *ABCA1* and *apoE*. Treatment of AD mice with either compound has been shown to improve memory and reduce brain Aβ levels, particularly hippocampal Aβ42 (13, 14, 28–30). Importantly, beneficial effects could be observed after only 6–7 days of treatment (28, 29), suggesting that stimulation of LXR-responsive genes may be of interest as a therapeutic approach for symptomatic AD.

However, existing LXR agonists have the unavoidable side effect of activating fatty acid synthase and sterol response element-binding protein-1c in the liver, which leads to hypertriglyceridemia and hepatic steatosis, particularly in species such as humans that express cholesterol ester transfer protein (31). Although LXR agonists such as GW3965 can safely be used in mice, which lack cholesterol ester transfer protein, LXR agonists have not yet been evaluated in humans. As a result, the therapeutic potential of LXR agonists remains untapped.

Determining which LXR target genes mediate the beneficial effects of LXR agonists on behavior and neuropathology may offer insights into new strategies that avoid the undesirable side effects of current compounds. Therefore, the objective of this study was to assess the specific contribution of *ABCA1* in the beneficial response to LXR agonists in APP/PS1 mice, an established model of amyloidogenesis, which co-express both APP and presenilin 1 (PS1) transgenes (37). We generated female APP/PS1 mice with and without functional *ABCA1* and treated individual cohorts with the LXR agonist GW3965 using low dose (2.5 mg/kg/day) prophylactic, low dose (2.5 mg/kg/day) therapeutic, and high dose (33 mg/kg/day) therapeutic treatment arms. We report that *ABCA1* contributes to both behavioral and biochemical end points in response to GW3965.

EXPERIMENTAL PROCEDURES

Animals and GW3965 Treatment—APP/PS1 (line 85) mice (Jackson Laboratories) co-express two transgenes from the murine prion promoter: a chimeric mouse/human APP650 cDNA containing the Swedish (K670M/N671L) mutations, and the human PS1 gene deleted for exon 9 (32). APP/PS1 mice are maintained on a mixed F1 C3H/H3J × C57Bl/6 background and develop thioflavin S-positive amyloid deposits at 36–40 weeks of age (32). $ABCA1^{-/-}$ mice (Jackson Laboratories) are on a mixed DBA/C57Bl/6 background (33) and are maintained by heterozygous matings. *ABCA1*-deficient APP/PS1 mice were generated by crossing APP/PS1 mice $ABCA1^{-/-}$ mice followed by one backcross. $ABCA1^{+/+}$ littermates were generated using a similar backcrossing strategy to control for admixture of genetic background in experimental cohorts. Animals were randomized into four study arms, each containing $n = 10$–19 APP/PS1 or $n = 4$–13 APP/PS1/$ABCA1^{-/-}$ female mice. Animals in the control groups were fed a standard chow diet (PMI LabDiet 5010, containing 24% protein, 5.1% fat, and 0.03% cholesterol). Treated groups were fed chow in which GW3965 was compounded (Research Diets) at 10 mg/kg to result in an average dose of 2.5 mg/kg/day/mouse (low dose) or at 120 mg/kg to result in an average dose of 33 mg/kg/day/mouse (high dose). Mice in the prophylactic group were treated with 2.5 mg/kg/day of GW3965 from 16 weeks up to 40 weeks of age (24-week duration), whereas mice in the therapeutic groups were treated from 32 to 40 weeks of age (8 week duration). Behavioral analyses were performed at 40 weeks of age after which animals were sacrificed. All procedures involving animals were approved by the Canadian Council of Animal Care and the University of British Columbia Committee on Animal Care.

Behavioral Testing—Animals were housed for 10 days prior to behavioral testing in a quiet room with a reversed 12-h dark/12-h light cycle. All testing was performed during the dark cycle.

Novel Object Recognition—The novel object recognition task, which uses cortical and hippocampal inputs, was administered as described (34, 35). The objects to be discriminated were made of biologically neutral materials and weighted to prevent movement in the open field. Twenty-four hours prior to training, mice were habituated to an empty open field (14 × 24 × 14 inch) for 10 min. During training, mice were placed in the center of the open field, which did not contain shavings, in a brightly lit testing room. The time spent exploring two identical objects (yellow, plastic duck-shaped toys) located in the north and south quadrant, spaced equidistant from the walls and animal, was quantified. The definition of exploring was that the

mouse was sniffing, climbing on, or touching the object and was a body length or less away from the object (*i.e.* less then 3 cm) while facing the object or orientated toward it. Trials were tracked using an overhead digital camera and analyzed using the ANY-maze video tracking software (Stoelting). Between each trial, the open field was cleaned with 70% ethanol to eliminate olfactory cues. Four hours after training, mice were tested. For testing, one of the identical objects was replaced with a novel object (purple, plastic hippopotamus-shaped toy) of similar size. The side of the open field with the novel object was alternated for each mouse to avoid a side preference. The time spent exploring the identical and novel objects were recorded. An increased percentage of time spent exploring the novel object (duration spent with novel object/(duration spent with novel object + duration spent with familiar object) × 100) is considered an index of enhanced cognitive performance in this task. The training and testing trails were each 5 min long.

Morris Water Maze—Hippocampal-dependent spatial memory was examined using the Morris water maze (MWM) (36). The water maze consisted of a plastic pool (100 cm in diameter and 54 cm high). An overhead video camera coupled to a computer and tracking software (ANY-maze video tracking system, Stoelting) was used to track movements. The water remained a constant temperature of 22–25 °C and was made opaque with non-toxic, water-based, white tempera paint. Distinct geometric shapes were attached to the walls of the pool on three sides, and the experimenter and computer system were hidden. Mice were assessed for latency to find a hidden platform that remained in the same quadrant of the pool for the entire training period. The training consisted of four blocks of trials (4 trials/block, with a 5-min trial interval). Each trial lasted until the mouse climbed onto the hidden platform within 60 s, and the escape latency onto the platform was recorded.

Cerebrospinal Fluid and Tissue Collection—Mice were fasted for 4 h prior to anesthetization with a mixture of 20 mg/kg of xylazine (Bayer) and 150 mg/kg of ketamine (Bimeda-MTC) via intraperitoneal injection. Cerebrospinal fluid (CSF) was collected as described (37). Approximately 15 μl was obtained from each mouse. Mice were then transcardially perfused with phosphate-buffered saline (PBS) for 7 min. Brains were removed and divided into right and left hemispheres. Cortex and hippocampus were dissected from the right hemisphere and kept frozen at −80 °C until analysis. The left hemisphere was immersion-fixed in 10% neutral buffered formalin for at least 48 h and cryoprotected in 30% sucrose in PBS at 4 °C.

Protein Extraction—Tissues were homogenized in ~8 volumes (cortex 500 μl, hippocampus 250 μl) of ice-cold carbonate buffer (100 mM Na_2CO_3, 50 mM NaCl, pH 11.5) containing Complete protease inhibitor (Roche Applied Science) in a Tissuemite homogenizer at full speed for 20 s. The homogenate was sonicated at 20% output for 10 s, then centrifuged at 4 °C for 45 min at 12,500 × g in a microcentrifuge (Eppendorf). The supernatant (carbonate-soluble fraction) was removed and neutralized by adding ~1.5 volumes of 1 M Tris, pH 6.8, to give a solution with a final pH ~7.4. This fraction was then used to evaluate *apoE*, *ABCA1*, APP, APP-CTFs, and $A\beta$. The pellet (carbonate insoluble fraction) was resuspended in an equal amount of 5 M guanidine hydrochloride in 50 mM Tris-HCl, pH

8.0, at room temperature for 2.5–3 h with continuous rotation to evaluate plaque-associated $A\beta$. Brain tissue from all animals was extracted in an identical manner, and all fractions were aliquoted and immediately frozen at −80 °C until analysis. Protein concentration was determined by DC Protein assay (Bio-Rad).

Western Blot Analysis of ABCA1, ApoE, APP, and APP-CTF—For analysis of *ABCA1*, *apoE*, and APP, 50 –100 μg of carbonate lysate was electrophoresed through 10% SDS-polyacrylamide gels, transferred to PVDF membrane (Millipore), and immunodetected using a monoclonal anti-*ABCA1* antibody, AC10 (1:1000, a kind gift from Dr. M. R. Hayden), a murine-specific *apoE* antibody (1:1000, Santa Cruz Biotechnology), an anti-APP antibody that recognizes both murine and human APP (clone 22C11, 1:2000, Chemicon), or an anti-actin antibody (1:5000, Chemicon) as a loading control. APP and APP-CTF were analyzed by resolving 25 μg of carbonate lysate through 4–12% NuPAGE BisTris gradient gels (Invitrogen, NP0335). Following transfer to a PVDF membrane, blots were probed using an anti-APP-CTF antibody (1:2000, Sigma), 22C11 or anti-actin. Blots were developed using enhanced chemiluminescence (Amersham Biosciences) according to the manufacturer's recommendations and quantitated using densitometry. Films were scanned into TIFF format at 600 dpi resolution and pixel counts were determined using ImageJ (NIH) software. Levels of *ABCA1*, *apoE*, APP, and APP-CTF were normalized to actin and expressed as fold-difference compared with non-treated APP/PS1 controls. For APP, values obtained from SDS-PAGE and BisTris Western blots were averaged. Each mouse was analyzed at least in duplicate, using independent gels run on different days with different ordering of samples to avoid edge effects and different pairings to avoid bias. For *ABCA1* and *apoE* quantitations, each sample was evaluated on at least 2 independent gels.

Western Blot Analysis of CSF—For analysis of CSF *apoE* particles, 10 μl of CSF was pooled from two mice and electrophoresed through 6% native polyacrylamide gels, transferred to PVDF membrane (Millipore), and immunodetected using an *apoE* antibody (1:500, Chemicon) followed by an anti-albumin antibody (1:2000, Bethyl Laboratories) as a loading control. Blots were developed using enhanced chemiluminescence (Amersham Biosciences) according to the manufacturer's recommendations.

Dot Blot Analysis of Total and Oligomeric $A\beta$—2 to 4 μg of cortical carbonate soluble lysate was spotted onto a dry nitrocellulose membrane and allowed to absorb. Following rehydration in 20% methanol and blocking in a solution of 5% milk in TBS, blots were probed with a monoclonal antibody against amino acid residues 1–17 of $A\beta$ (1:1000, clone 6E10, Chemicon) to detect total $A\beta$ or an anti-oligomeric antibody (1:1000, clone A11, BIOSOURCE) to detect oligomeric $A\beta$. Blots were developed and quantitated as above. Levels of oligomeric $A\beta$ were normalized to total $A\beta$ for each individual mouse and expressed as fold-difference compared with non-treated APP/PS1 controls.

$A\beta$ ELISA—$A\beta40$ and $A\beta42$ ELISAs were performed using commercial kits (KHB3442/KHB3441, BIOSOURCE) following the manufacturer's instructions. Carbonate soluble and
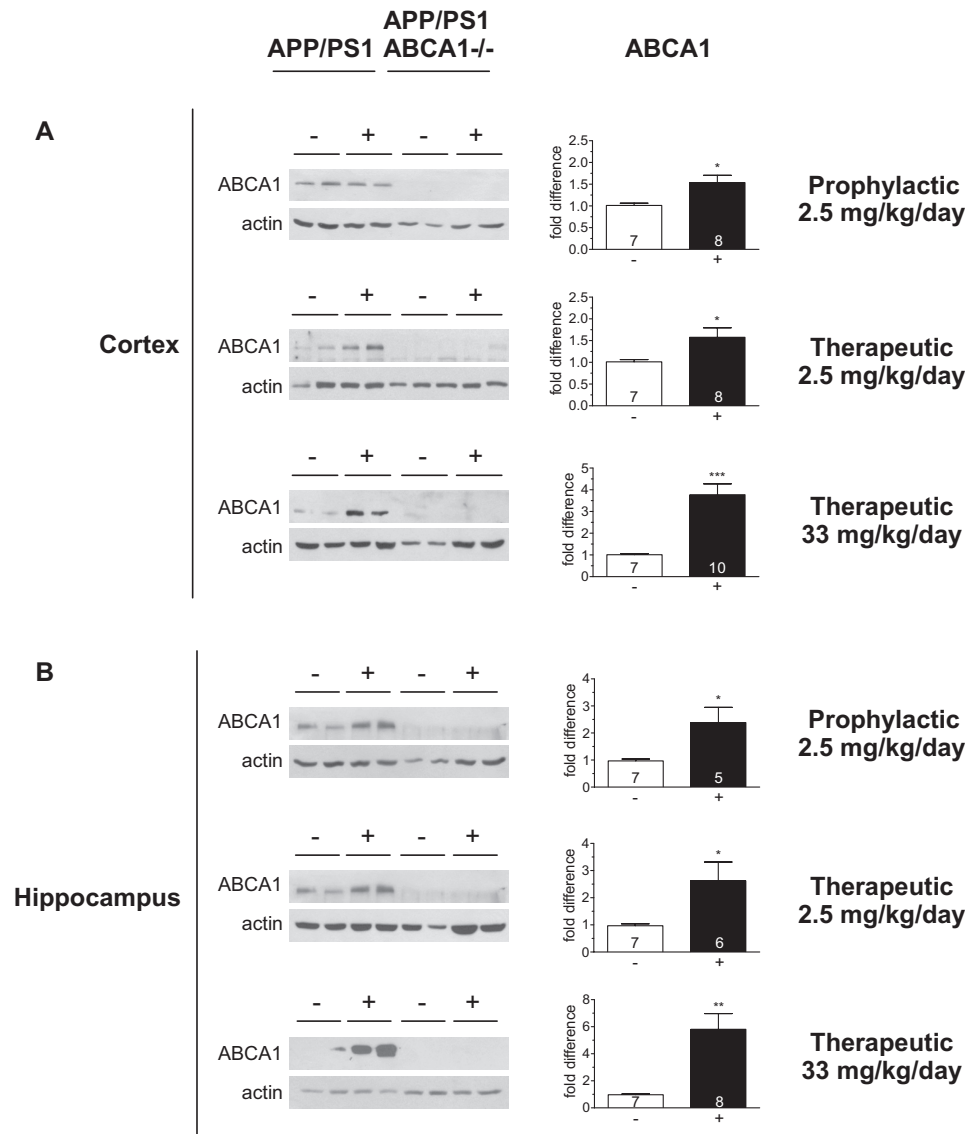
FIGURE 1. ***ABCA1 protein levels reflect GW3965 dose.*** Cortical and hippocampal extracts from untreated (−: *black*) and treated (+: *white*) mice were immunoblotted for *ABCA1*. *Left panels* are representative blots using undiluted samples from individual mice from the following cohorts: APP/PS1 untreated control: $n = 7$ (cortex), $n = 7$ (hippocampus); APP/PS1 prophylactic: $n = 8$ (cortex) $n = 5$ (hippocampus); APP/PS1 low dose therapeutic: $n = 8$ (cortex), $n = 6$ (hippocampus); APP/PS1 high dose therapeutic: $n = 10$ (cortex), $n = 9$ (hippocampus); $ABCA1^{-/-}$ APP/PS1 untreated control: $n = 4$ (cortex), $n = 4$ (hippocampus); $ABCA1^{-/-}$ APP/PS1 prophylactic: $n = 8$ (cortex) $n = 8$ (hippocampus): $ABCA1^{-/-}$ APP/PS1 low dose therapeutic: $n = 8$ (cortex), $n = 8$ (hippocampus); $ABCA1^{-/-}$ APP/PS1 high dose therapeutic: $n = 4$ (cortex), $n = 4$ (hippocampus). Samples from each mouse were normalized to actin and expressed as fold-difference compared with *ABCA1* levels in untreated APP/PS1 controls. Data represent mean ± S.E., where * represents $p < 0.05$, ** represents $p < 0.01$, and *** represents $p < 0.001$ by Students *t* test.

insoluble lysates were analyzed diluted in reaction buffer supplied by the manufacturer. Levels of $A\beta40$ and $A\beta42$ were normalized to total protein concentration.

Histology—25-μm thick, coronal sections were cut on a cryostat from fixed brains from the genu of the corpus callosum to the most caudal hippocampus. Sections were immersed for 10 min in 1% thioflavin S solution followed by washing and dehydration in increasing ethanol concentrations from 70 to 10% followed by xylene. Slides were mounted in dibutyl phthalate xylene mounting medium (DBH) and visualized within 24 h. Quantification of amyloid load was performed from six half-brain sections, 300 μm apart, spanning the entire length of the

hippocampus. Each section was compiled of 15 stitched images at ×4 magnification. This systematic sampling strategy was chosen to account for subregional variations of hippocampal size and potential variations in plaque burden. Images were viewed via FITC fluorescence using a BX61 microscope and quantitated using Image Pro (Media cybernetics) software. Areas of the regions of interest were outlined manually. The plaque/amyloid area within the field of interest (hippocampus or entire half-brain) was identified by color and intensity level threshold, this level was maintained throughout the experiment. Amyloid load (defined as the sum of thioflavin S staining area measured/sum of field analyzed × 100) was calculated for each section and then averaged across sections for each individual mouse. Images were quantitated automatically by Image Pro software.

Statistical Analysis—Results were analyzed using GraphPad (version 5.0). Treated cohorts were compared with their corresponding untreated control arm of the same genotype. Biochemistry results, including Western blots and $A\beta$ ELISA, were analyzed by one-way analysis of variance followed by a Tukey post test or, where indicated, two-tailed unpaired Student's *t* test. Student's *t* test was used for NOR, and two-way analysis of variance followed by a Bonferroni post test was used for MWM.

RESULTS

GW3965 Increases ABCA1 and ApoE Protein Levels in a Dose-dependent Manner but Does Not Affect APP Levels—Four treatment groups were generated for both APP/PS1 and *ABCA1*-deficient APP/PS1 cohorts. The first group consisted of untreated APP/PS1 and *ABCA1*-deficient APP/PS1 mice to serve as baseline controls for disease progression in the presence and absence of *ABCA1*. The second group consisted of pre-symptomatic APP/PS1 and *ABCA1*-deficient APP/PS1 mice treated prophylactically with low dose (2.5 mg/kg/day) GW3965, beginning at 16 weeks of age, for a total duration of 24 weeks. The remaining groups consisted of symptomatic APP/PS1 and *ABCA1*-deficient APP/PS1 mice treated therapeutically with low dose (2.5 mg/kg/day) or high dose (33 mg/kg/
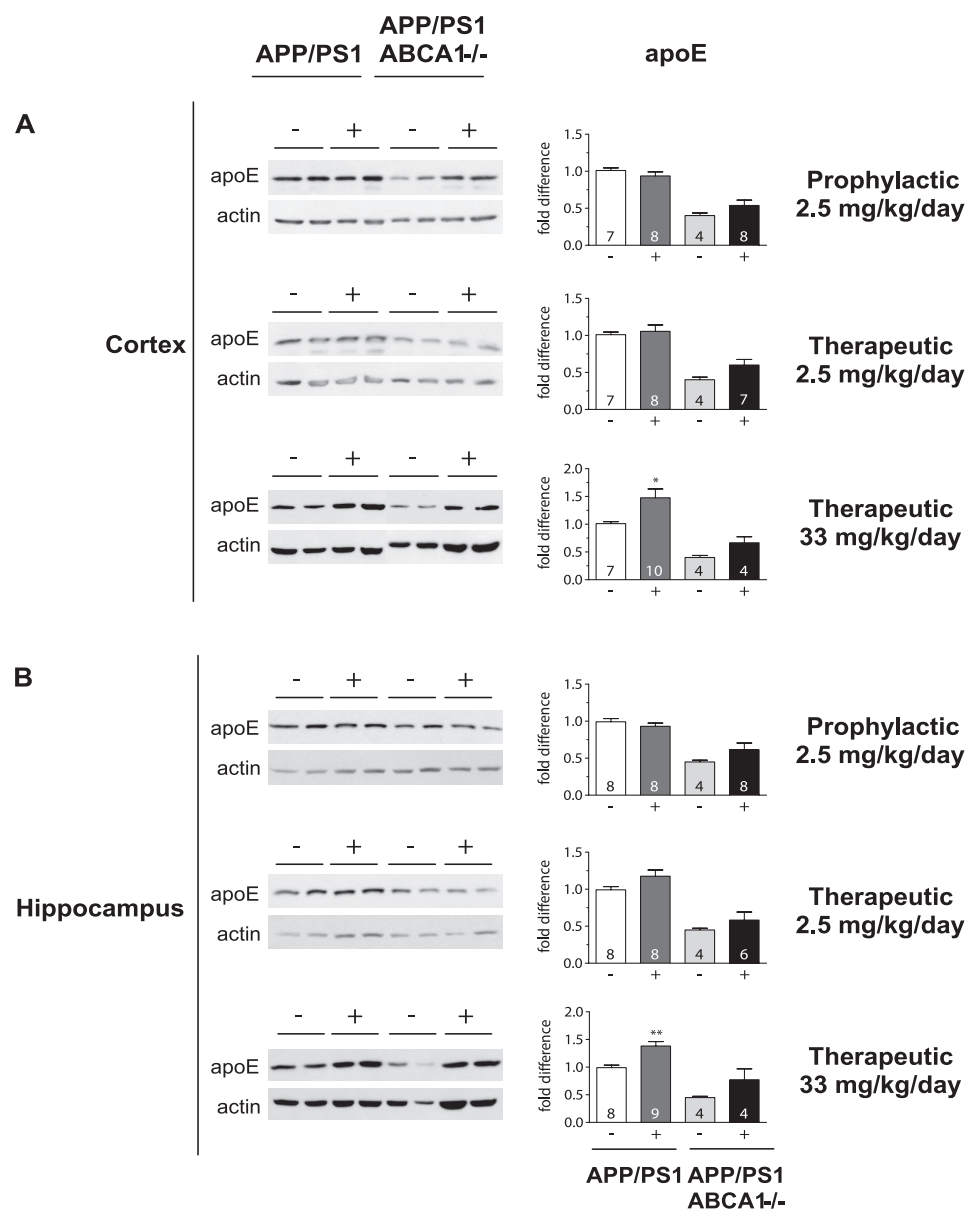
FIGURE 2. **High dose GW3965 is required for elevated *apoE* levels in tissue.** Cortical and hippocampal extracts from APP/PS1 untreated (−: *white*), APP/PS1 treated (+: *dark gray*), APP/PS1 *ABCA1*−/− untreated (−: *light gray*), and APP/PS1 *ABCA1*−/− treated (+: *black*) mice were immunoblotted for *apoE*. *Left panels* are representative blots using undiluted samples from individual mice from the following cohorts: APP/PS1 untreated control: $n = 7$ (cortex), $n = 8$ (hippocampus); APP/PS1 prophylactic: $n = 8$ (cortex) $n = 8$ (hippocampus); APP/PS1 low dose therapeutic: $n = 8$ (cortex), $n = 8$ (hippocampus); APP/PS1 high dose therapeutic: $n = 10$ (cortex), $n = 9$ (hippocampus); *ABCA1*−/− APP/PS1 untreated control: $n = 4$ (cortex), $n = 4$ (hippocampus); *ABCA1*−/− APP/PS1 prophylactic: $n = 8$ (cortex) $n = 8$ (hippocampus): *ABCA1*−/− APP/PS1 low dose therapeutic: $n = 7$ (cortex), $n = 6$ (hippocampus); *ABCA1*−/− APP/PS1 high dose therapeutic: $n = 4$ (cortex), $n = 4$ (hippocampus). Samples from each mouse were blotted at least twice, normalized to actin, and expressed as fold-difference compared with *apoE* levels in untreated APP/PS1 controls. Data represent mean ± S.E., where * represents $p < 0.05$ and ** represents $p < 0.01$ by one-way analysis of variance followed by Tukey post test.

2.6-fold ($n = 7$ control, 6 treated, $p < 0.01$), and 5.8-fold ($n = 7$ control, 8 treated, $p < 0.001$) increase in *ABCA1* protein levels in hippocampus (Fig. 1 and supplemental Fig. S1). Compared with *ABCA1*, *apoE* is less responsive to GW3965 and *apoE* protein levels were significantly increased only in the high dose therapeutic group with functional *ABCA1* in both cortex (1.5 fold, $n = 7$ control, 10 treated, $p < 0.05$) and hippocampus (1.4-fold, $n = 8$ control, 9 treated, $p < 0.01$) in treated APP/PS1 mice relative to untreated APP/PS1 controls (Fig. 2).

As predicted from previous studies, *apoE* protein levels were significantly lower by ∼60% ($n = 4$ control, $p < 0.001$) in all *ABCA1*-deficient animals, as poorly lipidated *apoE* is rapidly catabolized. Because *apoE* is independently activated by GW3965, we observed a subtle but insignificant increase in *apoE* protein levels in GW3965-treated *ABCA1*−/− animals. However, no treatment strategy achieved statistically significant increases in *apoE* protein levels in *ABCA1*-deficient APP/PS1 mice relative to untreated *ABCA1*-deficient APP/PS1 controls, nor restored *apoE* protein levels in any *ABCA1*−/− group to the wild-type levels observed in untreated APP/PS1 mice. These results suggest that increased transcription of *apoE* mRNA may be offset by catabolism of poorly lipidated *apoE* protein in *ABCA1*-deficient animals, leading to a trend but not a significant increase in steady state *apoE* protein levels in response to GW3965 treatment.

As expected, neither *ABCA1* deficiency nor GW3965 treatment significantly altered total APP levels in either hippocampus or cortex (supplemental Fig. S2), confirming that LXR agonists do not alter APP abundance. Previous studies have demonstrated that carboxyl-terminal fragments (CTF) of APP impair calcium homeostasis and learning and memory and are an important toxic component in the neuropathy of AD (38). Intriguingly, we observed a trend toward increased CTFα and CTFβ levels only in the hippocampus of mice treated with 33 mg/kg/day of GW3965 (supplemental Fig. S3), suggesting the possibility that APP processing may be affected at this dose. Levels of CTF were

day) GW3965, beginning at 32 weeks of age, for a total duration of 8 weeks. All animals were analyzed at 40 weeks of age.

Western blot analysis of cortical and hippocampal tissue revealed that low dose prophylactic, low dose therapeutic, and high dose therapeutic treatment with GW3965 led to a significant 1.5-fold ($n = 7$ control, 8 treated, $p < 0.05$), 1.6-fold ($n = 7$ control, 8 treated, $p < 0.05$), and 3.8-fold ($n = 7$ control, 10 treated, $p < 0.001$) increase in *ABCA1* protein levels in cortex, and a significant 2.4-fold ($n = 7$ control, 5 treated, $p < 0.05$),
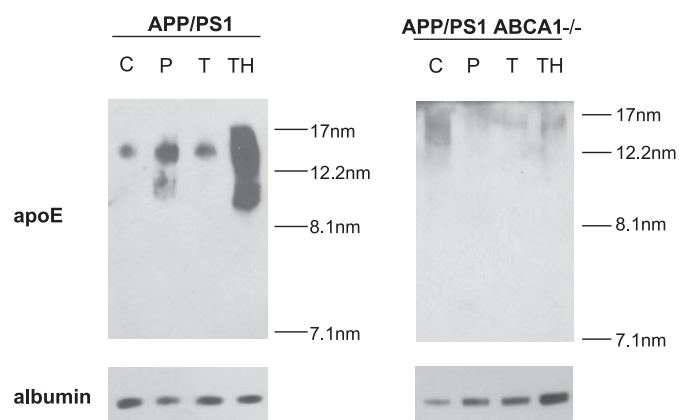
FIGURE 3. **ABCA1 is required for increased CSF *apoE* levels in response to GW3965.** Equal volumes of CSF from individual mice from untreated control (*C*), prophylactic (*P*), low dose therapeutic (*T*), and high dose therapeutic (*TH*) groups of APP/PS1 and APP/PS1 *ABCA1*$^{-/-}$ mice were pooled, separated by 6% native PAGE, and immunoblotted for *apoE* and albumin. Stokes diameter markers are shown on the *right*.

not altered at low dose GW3965 treatment or upon deletion of *ABCA1*.

ABCA1 Is Required to Observe Increased CSF apoE in Response to GW3965—Immunoblot analysis of CSF showed that treatment of APP/PS1 mice with functional *ABCA1* with 2.5 mg/kg/day of GW3965 have slightly increased CSF *apoE* levels (Fig. 3), consistent with modestly elevated *apoE* protein in tissue. APP/PS1 animals receiving 33 mg/kg/day of GW3965 exhibited a dramatic, ~10-fold, increase in lipidated CSF *apoE* particles. CSF *apoE* levels in *ABCA1*-deficient mice are ~20-fold lower than in wild-type animals, and therefore as expected from these previous studies, untreated *ABCA1*-deficient APP/PS1 mice displayed greatly reduced CSF *apoE* levels relative to APP/PS1 controls. Furthermore, *ABCA1*-deficient APP/PS1 animals completely failed to exhibit elevated *apoE* levels in CSF under any treatment strategy.

High Dose GW3965 Shifts Aβ from Guanidine to Soluble Pools Independent of ABCA1—Proteolytic cleavage of APP by β-secretase initiates the production of soluble, monomeric Aβ peptides that aggregate to form the insoluble, fibrillar form of Aβ commonly found in senile plaques. In APP/PS1 mice with functional *ABCA1*, low dose (2.5 mg/kg/day) GW3965 had little effect on carbonate-soluble or guanidine-soluble (fibrillar) pools of Aβ40 and Aβ42 in the cortex and hippocampal regardless of prophylactic (24 weeks) or therapeutic (8 weeks) treatment duration (Fig. 4). The only exception to this observation that reached statistical significance was an increase in hippocampal carbonate-soluble Aβ42 (2.9-fold, $p < 0.05$) in APP/PS1 mice receiving 2.5 mg/kg/day of GW3965 for 8 weeks (therapeutic group). In *ABCA1*-deficient APP/PS1 mice, low dose GW3965 tended to increase Aβ40 and Aβ42 levels in both carbonate- and guanidine-soluble pools in both cortex and hippocampus, particularly in animals in the therapeutic arm, although no increase reached statistical significance. These observations are consistent with previous studies showing that that loss of *ABCA1* does not markedly affect baseline Aβ levels (7, 8, 11, 14) and that less than 30 mg/kg/day of the LXR agonist TO901317 for 7 days does not alter Aβ levels in Tg2576 mice (29).

APP/PS1 mice treated with high dose (33 mg/kg/day) GW3965 for 8 weeks showed elevated carbonate-soluble Aβ40 and Aβ42 in both cortex and hippocampus. Specifically, carbonate-soluble Aβ40 levels were increased in the cortex (5.2-fold, $p < 0.01$) and hippocampus (3.0-fold, $p < 0.001$), whereas carbonate-soluble Aβ42 levels were increased in the cortex (1.9-fold, $p < 0.001$) and showed a trend toward elevated levels in the hippocampus (2.3-fold, $p > 0.05$). In these animals, Aβ levels in the corresponding cortical guanidine-soluble fractions tended to decrease, although no decrease reached statistical significance. Similar trends were observed in *ABCA1*-deficient APP/PS1 mice treated with high dose GW3965, however, the only significant increase compared with untreated genotype-matched controls was for carbonate-soluble Aβ40 in the cortex (3.6-fold, $p < 0.001$). These observations suggest that treatment of APP/PS1 mice with a high dose of GW3965 may promote the retention of Aβ in soluble rather than deposited pools irrespective of *ABCA1*.

Because neurotoxicity has been suggested to correlate better with oligomeric rather than total Aβ levels (39), we performed dot blot experiments on carbonate-soluble cortical extracts using the oligomer-specific A11 antibody and the 6E10 antibody that detects all forms of Aβ. Animals treated with high dose GW3965 showed a balanced increase in oligomeric and total Aβ, which resulted in no net change in the A11:6E0 ratio irrespective of *ABCA1* (supplemental Fig. S4). Although animals treated with low dose GW3965 showed no significant changes in oligomeric or total Aβ, we noted that the A11:6E10 ratio was significantly elevated in the *ABCA1*-deficient APP/PS1 cohort treated for 8 weeks with 2.5 mg/kg/day of GW3965, which is likely due to a non-significant decease in total Aβ detected on a dot blot. The most conservative conclusion from this experiment is that neither GW3965 treatment nor *ABCA1* genotype affects the relative amount of Aβ oligomers.

ABCA1 Is Required for a GW3975-mediated Reduction in Amyloid Burden—Thioflavin-S histology revealed that GW3965 tended to reduce the amyloid load in the hippocampus and whole brain in the treated APP/PS1 cohorts examined here (Fig. 5). In contrast, *ABCA1*-deficient APP/PS1 animals failed to exhibit lowered amyloid levels when treated with high dose GW3965 in whole brain and showed a clear trend toward increased hippocampal amyloid load that was significant in animals receiving 33 mg/kg/day of GW3965. These observations suggest that *ABCA1* contributes to the reduced amyloid burden in response to GW3965 treatment.

ABCA1 Deficiency Compromises Gains in Cognitive Function in APP/PS1 Mice Treated with GW3965—To determine whether *ABCA1* contributes to improved cognition upon GW3965 treatment, we evaluated APP/PS1 mice with and without *ABCA1* in both novel object recognition (NOR) and MWM tasks relative to wild-type strain-matched controls (Fig. 6). Each treatment strategy showed consistent results in the NOR. All animals showed equivalent responses in the training phase of this task, indicating that the presence of Aβ or the absence of *ABCA1* did not affect baseline exploratory behavior. As expected, wild-type animals showed a significant preference for novelty, spending ~60% of their time exploring the novel
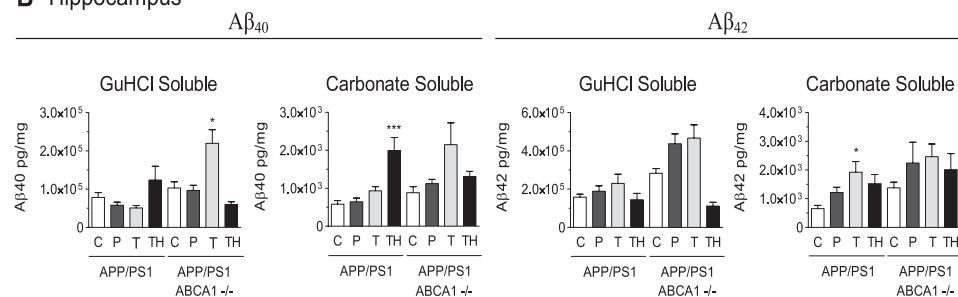
A Cortex
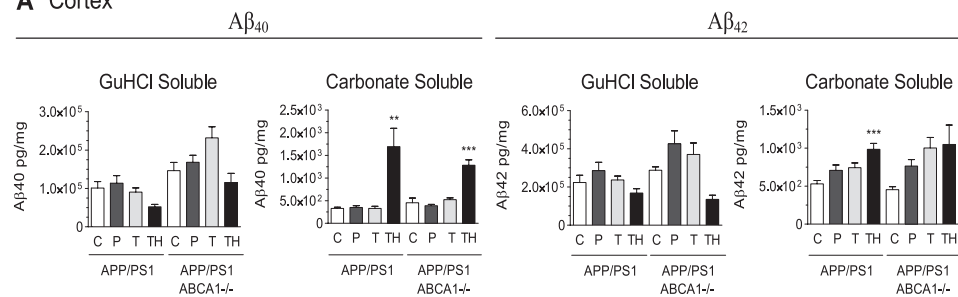
B Hippocampus

FIGURE 4. **Effect of GW3965 and *ABCA1* on cortical and hippocampal Aβ levels.** Tissues were serially extracted with carbonate followed by guanidine hydrochloride and Aβ40 and Aβ42 levels in each fraction were measured by ELISA. Data represent mean ± S.E. of 1–4 measurements from each mouse. Cohorts consisted of the following Ns: APP/PS1 untreated control: $n = 7$ (cortex), $n = 8$ (hippocampus); APP/PS1 prophylactic: $n = 8$ (cortex) $n = 8$ (hippocampus); APP/PS1 low dose therapeutic: $n = 8$ (cortex), $n = 8$ (hippocampus); APP/PS1 high dose therapeutic: $n = 10$ (cortex), $n = 10$ (hippocampus); $ABCA1^{-/-}$ APP/PS1 untreated control: $n = 4$ (cortex), $n = 4$ (hippocampus); $ABCA1^{-/-}$ APP/PS1 prophylactic: $n = 8$ (cortex) $n = 8$ (hippocampus); $ABCA1^{-/-}$ APP/PS1 low dose therapeutic: $n = 8$ (cortex), $n = 8$ (hippocampus); $ABCA1^{-/-}$ APP/PS1 high dose therapeutic: $n = 4$ (cortex), $n = 4$ (hippocampus). Data represent mean ± S.E., where * represents $p < 0.05$, ** represents $p < 0.01$, and *** represents $p < 0.001$ by one-way analysis of variance followed by Tukey post test. *C*, control; *P*, prophylactic; *T*, low dose therapeutic; *TH*, high dose therapeutic.

object ($p = 0.001$), whereas untreated APP/PS1 mice were considerably impaired and explored the known object as frequently as the novel one. All treatments significantly improved cognitive performance of APP/PS1 mice nearly to wild-type levels (prophylactic GW3965, $p = 0.047$; low dose therapeutic GW3965, $p = 0.001$; high dose therapeutic GW3965, $p = 0.0001$), demonstrating that the hippocampal and perirhinal cortical pathways are important for NOR (40) to respond positively to LXR agonists even after the onset of amyloid deposition. Notably, no treatment strategy was able to achieve significant improvements in NOR performance of *ABCA1*-deficient APP/PS1 mice and these animals were nearly as impaired as untreated APP/PS1 mice in each of the treatment groups.

In the MWM task, wild-type mice readily learned the location of the platform, whereas untreated APP/PS1 mice did not show any significant decrease in escape latency over 4 days of trials. Wild-type mice performed significantly better than untreated APP/PS1 mice on day 4 ($p < 0.001$). Treatment of APP/PS1 mice with GW3965 in both prophylactic and low dose therapeutic arms improved MWM performance, which initially was similar to wild-type animals over the first 3 trials and reached an intermediate performance level significantly different from both wild-type ($p < 0.05$) and untreated APP/PS1 mice ($p < 0.05$) on the 4th day. The performance of APP/PS1 mice treated with high dose GW3965 was similar to wild-type mice on each trial day ($p > 0.05$) and significantly

improved over untreated APP/PS1 mice on days 3 and 4 ($p < 0.01$).

ABCA1 deficiency had subtler effects on MWM performance than for the NOR task. In both prophylactic and low dose therapeutic groups, *ABCA1*-deficient APP/PS1 mice displayed similar latency times as similarly treated APP/PS1 controls. The impact of *ABCA1* deficiency was evident only upon high dose therapeutic treatment, where lack of *ABCA1* was associated with significantly poorer performance on all days except day 3. On day 4, the performance of *ABCA1*-deficient APP/PS1 mice treated with high dose GW3965 was similar to untreated APP/PS1 mice ($p > 0.05$), and significantly poorer than treated APP/PS1 and wild-type animals ($p < 0.001$). These results suggest that neuronal circuits required for improvement in the MWM task may be less responsive to LXR agonists compared with NOR, as only high dose treatment improved MWM performance of APP/PS1 mice to approach that of wild-type animals, and the effect of *ABCA1* deficiency was observed only in the high dose arm.

DISCUSSION

LXR agonists have clear beneficial effects on both cognitive and biochemical end points in AD mice. Koldamova *et al.* (28) showed that 11-week-old APP23 mice treated for 6 days with 50 mg/kg/day of TO901317 displayed increased ABCA1 expression, no change in *apoE* levels, decreased RIPA-soluble Aβ40 and Aβ42 levels, and a shift in APP processing from β- to α-secretase cleavage. Riddel *et al.* (29) showed that symptomatic 20-week-old Tg2576 mice treated for 7 days with 50 mg/kg/day of TO901317 displayed improved performance in contextual fear conditioning. *ABCA1* and *apoE* mRNA levels were increased to a greater extent in hippocampus compared with cortex in animals treated with 30 mg/kg/day of TO901317, accompanied by a selective decrease in guanidine-soluble hippocampal Aβ42 (29). Jiang *et al.* (13) treated 12-month-old symptomatic Tg2765 mice for 4 months with 33 mg/kg/day of GW3965 and observed increased *ABCA1* expression accompanied by a dramatic reduction in plaque load and decreased Aβ40 and Aβ42 levels, without altering APP processing. In this study, a 6-day treatment with 50 mg/kg/day of GW3965 was sufficient to fully restore performance in the contextual fear conditioning task (13). Vanmierlo *et al.* (30) treated 21-month-old APPSLxPS1 mice with 30 mg/kg/day of TO901317 and observed improved performance on both object memory and object location tasks with no alteration in amyloid load. Finally,
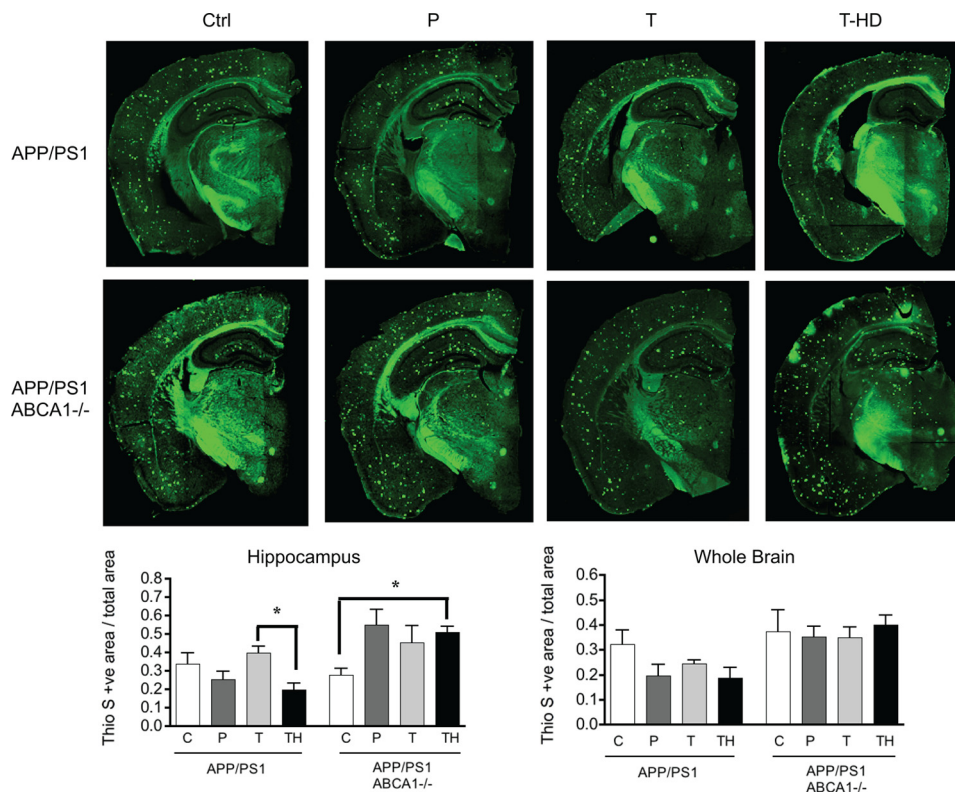
FIGURE 5. **High dose GW3965 solubilizes amyloid in APP/PS1 mice with functional *ABCA1*.** *top,* thioflavin-S staining of hemicoronal sections from APP/PS1 mice in the presence or absence of *ABCA1*, with or without GW3965 treatment. *Scale bar* represents 1000 μm. Amyloid load was quantitated in the hippocampus (*bottom left*) and whole hemi-brain (*bottom right*) as described under "Experimental Procedures." Values represent mean ± S.E. of total amyloid load from 6 hemi-coronal brain sections per mouse, n = 2–6 mice per group. *C*, control; *P*, prophylactic; *T*, low dose therapeutic; *TH*, high dose therapeutic.

Burns *et al.* (14) observed a dose-dependent increase in *ABCA1* and *apoE* expression concomitant with decreased endogenous murine Aβ42 levels in wild-type mice treated for 7 days with 50 mg/kg/day of TO901317. Furthermore, genetic deficiency of the LXR target gene *ABCA1* reduces *apoE* levels and lipidation in the central nervous system and exacerbates amyloidogenesis (6–9, 11), whereas selective overexpression of *ABCA1* by 6-fold or more is sufficient to nearly eliminate the formation of amyloid plaques (10). This body of work suggests that LXR agonists may promote beneficial responses in APP transgenic mice through *ABCA1*. The present study was therefore designed to address three questions: 1) do LXR agonists require *ABCA1* to produce beneficial outcomes in APP/PS1 mice; 2) how does the LXR agonist dose affect target gene induction, cognitive performance, and Aβ metabolism; 3) is prophylactic treatment superior to therapeutic treatment with respect to behavioral and biochemical end points? We therefore evaluated cognitive, biochemical, and neuropathological end points in female APP/PS1 mice, with and without *ABCA1*, that were treated with GW965 for different durations and at different doses. We selected females for our study as female APP/PS1 mice display a more severe accumulation of amyloid load and because women have an increased prevalence of AD compared with men.

We show that *ABCA1* is an important LXR target gene that contributes to several positive effects of LXR agonists in female APP/PS1 mice. Specifically, APP/PS1 animals lacking *ABCA1* completely failed to respond to GW3965 with respect to NOR performance and increased tissue and CSF *apoE* levels. *ABCA1* was also clearly implicated in the tendency to exhibit reduced amyloid load in GW3965-treated animals.

Cognitive performance in the NOR task was the most sensitive measure of improvement identified in this study, as treated APP/PS1 mice displayed equivalent *ABCA1*-dependent gains in object memory when treated with 2.5 or 33 mg/kg/day of GW3965. That *ABCA1*-dependent object recognition memory can be substantially improved in the absence of reduced Aβ or amyloid levels suggests that Aβ and amyloid deposits may not markedly affect cognitive function. Alternatively, *ABCA1* may play a particularly important role in promoting the clearance of Aβ pools that are critical for cognitive function, and that these pools may be distinct from carbonate- or guanidine-soluble Aβ, oligomeric Aβ, and mature amyloid. Our results are similar to those of Vanmierlo *et al.* (30), who reported significantly improved behavior in object recognition and object location tasks in APPSLxPS1 mice treated with 30 mg/kg/day of TO901317 for 6–9 weeks. Intriguingly, they also observed significant improvements in behavior without significant changes in amyloid burden. Our study, along with that of Vanmierlo *et al.* (30), suggests that clinical improvement in cognitive functioning in humans may be possible without necessarily reducing total Aβ or amyloid levels.

Unlike NOR, performance on the MWM task was not fully rescued with low dose GW3965 and required 33 mg/kg/day to reach wild-type performance on the 4th trial day. Object recognition tasks, like NOR, require cooperative function between hippocampal and perirhinal cortex (40), rather than reliance largely on hippocampal function for spatial memory involved in the MWM. Previous work by Riddell (13) and Jiang *et al.* (29) showed that performance of Tg2576 mice in a contextual fear conditioning task, which uses inputs from hippocampus and amygdala, also respond positively to LXR agonists. It would be interesting to determine whether there are other differential sensitivities to LXR agonists in behavioral tasks in these and other murine models of amyloid deposition, as such information could help to refine functional pathways that could benefit from therapies involving the *ABCA1-apoE* pathway.

We observed several dose-dependent effects of GW3965 in our study. *ABCA1* was up-regulated at lower doses than *apoE*, consistent with previous observations that *apoE* is less sensitive to LXR-mediated induction (13, 14, 29). Unlike previous reports in Tg2576 mice, we did not observe selective responses
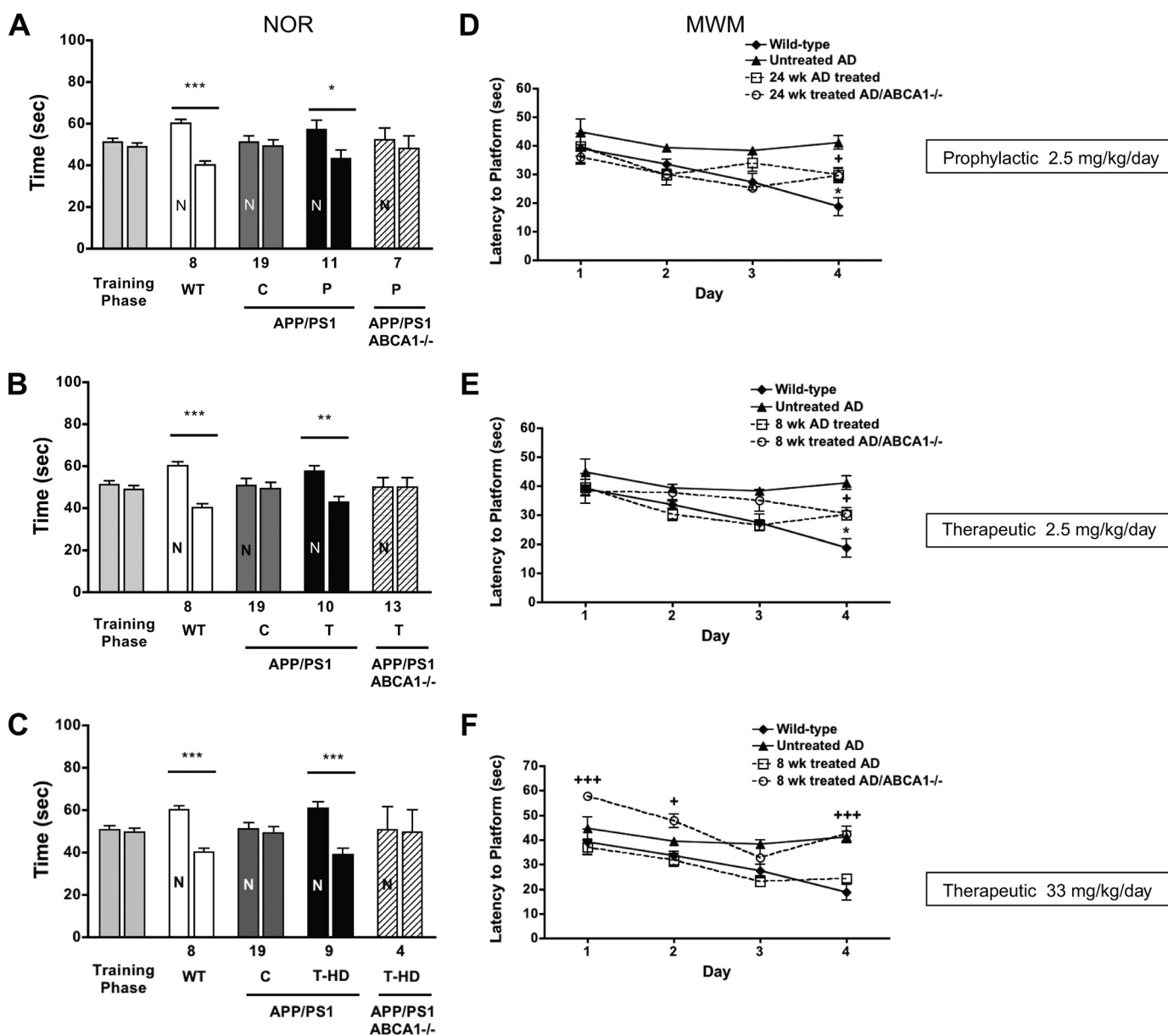
FIGURE 6. ***ABCA1 is required for LXR-mediated improvement in object but not spatial memory.*** *A–C*, percentage of NOR in APP/PS1 mice with and without *ABCA1* treated prophylactically with GW3965 for 24 weeks (*A*) or treated therapeutically at a low dose (*B*) or therapeutically at a high dose (*C*) for 8 weeks. Littermate controls include wild-type and untreated APP/PS1 animals. *N* represents the novel object, and cohort size is listed *below* the column. *D–F*, latency to locate a hidden platform in the MWM task in the same animals treated prophylactically (*D*) or therapeutically at a low dose (*E*) or therapeutically at a high dose (*F*) with GW3965. *Columns* represent the mean ± S.D. and, for the MWM task, are grouped into 4-day trial blocks. Cohort size for the MWM task are: wild-type, $n = 8$; untreated APP/PS1, $n = 19$; 24 weeks (prophylactic) APP/PS1 treated, $n = 11$; 24 weeks (prophylactic) APP/PS1/$ABCA1^{-/-}$ treated, $n = 8$; 8 weeks (therapeutic) APP/PS1 treated, $n = 11$; 8 weeks (therapeutic) APP/PS1/$ABCA1^{-/-}$ treated, $n = 11$. *** represents $p < 0.0001$; ** represents $p < 0.01$; * represents $p < 0.05$ comparing APP/PS1 treated to wild-type littermate controls. $+++$ represents $p < 0.001$; $++$ represents $p < 0.01$; $+$ represents $p < 0.05$ comparing APP/PS1/$ABCA1^{-/-}$ to wild-type littermate controls. *C*, control; *T*, low dose therapeutic.

of *ABCA1* in the hippocampus, perhaps reflecting differences among animal models, particularly if PS1 mutations are included as these have been implicated in bi-directional regulatory loops involving cholesterol and sphingomyelin homeostasis and APP processing (41). Low dose GW3965 did not affect total APP levels or processing in APP/PS1 mice, but high dose GW3965 led to a trend toward increased production of CTFα and CTFβ in hippocampus. Previously, Koldamova *et al.* (28) observed a shift in APP processing from β-secretase cleavage to α-secretase cleavage in Tg2576 mice treated with 50 mg/kg/day of TO901317, suggesting that high doses of LXR agonists may have some impact on APP processing.

Because LXR agonists activate a wide variety of genes in the brain (42), an important follow-up study will be to assess differential gene expression changes by LXR dose, which would be particularly informative for genes that influence inflammatory status. *ApoE* has a multitude of different functions and may contribute to lipid mobilization, Aβ clearance, and anti-inflammatory responses to LXR activation (43).

In APP/PS1 mice, the effect of GW3965 on Aβ levels and distribution between soluble and insoluble pools was markedly different from the reported effects for LXR agonists in the Tg2576 model. Previous studies with Tg2576 mice have demonstrated reduced hippocampal Aβ levels upon treatment with

TO901317 or GW3965. In contrast, APP/PS1 mice treated with 2.5 mg/kg/day of GW3965 had no change in Aβ levels other than a nonsignificant trend toward increased carbonate soluble Aβ42 in hippocampus. APP/PS1 receiving 33 mg/kg/day of GW3965 did show significantly increased carbonate soluble Aβ40 and Aβ42 in cortex- and carbonate-soluble Aβ40 in hippocampus, with similar trends observed in animals lacking *ABCA1*. However, none of the cohorts examined here displayed significant reductions in guanidine-soluble Aβ nor mature amyloid. Intriguingly, because the APPSLxPS1mut animals used by Vanmierlo *et al.* (30) also failed to exhibit significant reductions in deposited Aβ upon extended TO901317 treatment, it will be interesting to specifically examine the effect of the PS1 δ9 mutation in response to LXR agonists.

In vitro, lipidated *apoE* and *apoA-I* facilitate Aβ degradation by neprilysin and insulin degrading enzyme (13). Microglia efficiently take up and degrade soluble Aβ, and this process is enhanced if Aβ is added together with *apoA-I* or *apoE* (13). Neprilysin and related proteinases mediate intracellular degradation of soluble Aβ, whereas insulin degrading enzyme and related proteinases regulate Aβ degradation in the extracellular milieu (13). Importantly, loss of *apoE* or *ABCA1* activity greatly impairs the ability of primary microglia to degrade Aβ (13). An important question raised by our study is whether *ABCA1*-mediated lipidation of *apoE* clears Aβ via these proteinases *in vivo*, and whether the LXR dose affects insulin degrading enzyme or neprilysin levels or activity.

Interestingly, prophylactic treatment of asymptomatic APP/PS1 mice provided no advantage compared with therapeutic treatment of diseased APP/PS1 in any outcome measured. Indeed, therapeutic administration often led to subtly better responses with respect to tissue *apoE* levels and Aβ distribution. This observation is consistent with a previous example of a temporal response to LXR agonists. For example, cynomolgus monkeys treated with 10 mg/kg/day of GW3965 exhibited a transient increase in plasma LDL, TC, and apoB levels that peaked after 7 days of treatment and returned to baseline conditions by 14 days (31). It will be interesting to determine the temporal response of LXR target genes in brain and correlate these changes with improved cognitive function.

Our study used exclusively female APP/PS1 mice, whereas APPSLxPS1mut males were used by Vanmielo *et al.* (30) and Tg2576 males were used by Riddell *et al.* (29). The gender of the Tg2576 cohort investigated by Jiang *et al.* (13) is not reported. LXR agonists therefore consistently result in improved behavior across three different AD models, in either gender and with distinct agonists.

In conclusion, this study provides further support for the beneficial role LXR-responsive gene products have for beneficial effects on cognitive functions relevant for AD in multiple mouse models of amyloidogenesis. Furthermore, of the hundreds of genes activated by LXR agonists, our study is the first to specifically implicate *ABCA1* as a key component of this beneficial response, as without *ABCA1*, *apoE* cannot carry out its normal beneficial functions in the brain. Therefore, therapeutic strategies that specifically target *ABCA1* may be a viable approach for bypassing the deleterious side effects of existing LXR agonists for AD.

REFERENCES

1. Fan, J., Donkin, J., and Wellington, C. L. (2009) *Biofactors* **35,** 239–248
2. Morris, J. C. (1997) *Neurology* **49,** (suppl.) S7–S10
3. Yankner, B. A., and Lu, T. (2009) *J. Biol. Chem.* **284,** 4755–4759
4. Hardy, J. (1997) *Trends Neurosci.* **20,** 154–159
5. Bates, K. A., Verdile, G., Li, Q. X., Ames, D., Hudson, P., Masters, C. L., and Martins, R. N. (2009) *Mol. Psychiatry* **14,** 469–486
6. Hirsch-Reinshagen, V., Zhou, S., Burgess, B. L., Bernier, L., McIsaac, S. A., Chan, J. Y., Tansley, G. H., Cohn, J. S., Hayden, M. R., and Wellington, C. L. (2004) *J. Biol. Chem.* **279,** 41197–41207
7. Hirsch-Reinshagen, V., Maia, L. F., Burgess, B. L., Blain, J. F., Naus, K. E., McIsaac, S. A., Parkinson, P. F., Chan, J. Y., Tansley, G. H., Hayden, M. R., Poirier, J., Van Nostrand, W. E., and Wellington, C. L. (2005) *J. Biol. Chem.* **280,** 43243–43256
8. Wahrle, S. E., Jiang, H., Parsadanian, M., Hartman, R. E., Bales, K. R., Paul, S. M., and Holtzman, D. M. (2005) *J. Biol. Chem.* **280,** 43236–43242
9. Wahrle, S. E., Jiang, H., Parsadanian, M., Legleiter, J., Han, X., Fryer, J. D., Kowalewski, T., and Holtzman, D. M. (2004) *J. Biol. Chem.* **279,** 40987–40993
10. Wahrle, S. E., Jiang, H., Parsadanian, M., Kim, J., Li, A., Knoten, A., Jain, S., Hirsch-Reinshagen, V., Wellington, C. L., Bales, K. R., Paul, S. M., and Holtzman, D. M. (2008) *J. Clin. Invest.* **118,** 671–682
11. Koldamova, R., Staufenbiel, M., and Lefterov, I. (2005) *J. Biol. Chem.* **280,** 43224–43235
12. Koldamova, R. P., Lefterov, I. M., Lefterova, M. I., and Lazo, J. S. (2001) *Biochemistry* **40,** 3553–3560
13. Jiang, Q., Lee, C. Y., Mandrekar, S., Wilkinson, B., Cramer, P., Zelcer, N., Mann, K., Lamb, B., Willson, T. M., Collins, J. L., Richardson, J. C., Smith, J. D., Comery, T. A., Riddell, D., Holtzman, D. M., Tontonoz, P., and Landreth, G. E. (2008) *Neuron* **58,** 681–693
14. Burns, M. P., Vardanian, L., Pajoohesh-Ganji, A., Wang, L., Cooper, M., Harris, D. C., Duff, K., and Rebeck, G. W. (2006) *J. Neurochem.* **98,** 792–800
15. Dietschy, J. M., and Turley, S. D. (2001) *Curr. Opin. Lipidol.* **12,** 105–112
16. Ladu, M. J., Reardon, C., Van Eldik, L., Fagan, A. M., Bu, G., Holtzman, D., and Getz, G. S. (2000) *Ann. N. Y. Acad. Sci.* **903,** 167–175
17. Genest, J., Jr., Marcil, M., Denis, M., and Yu, L. (1999) *J. Investig. Med.* **47,** 31–42
18. Rust, S., Rosier, M., Funke, H., Real, J., Amoura, Z., Piette, J. C., Deleuze, J. F., Brewer, H. B., Duverger, N., Denèfle, P., and Assmann, G. (1999) *Nat. Genet.* **22,** 352–355
19. Bodzioch, M., Orsó, E., Klucken, J., Langmann, T., Böttcher, A., Diederich, W., Drobnik, W., Barlage, S., Büchler, C., Porsch-Ozcürümez, M., Kaminski, W. E., Hahmann, H. W., Oette, K., Rothe, G., Aslanidis, C., Lackner, K. J., and Schmitz, G. (1999) *Nat. Genet.* **22,** 347–351
20. Brooks-Wilson, A., Marcil, M., Clee, S. M., Zhang, L. H., Roomp, K., van Dam, M., Yu, L., Brewer, C., Collins, J. A., Molhuizen, H. O., Loubser, O., Ouellette, B. F., Fichter, K., Ashbourne-Excoffon, K. J., Sensen, C. W., Scherer, S., Mott, S., Denis, M., Martindale, D., Frohlich, J., Morgan, K., Koop, B., Pimstone, S., Kastelein, J. J., Genest, J., Jr., and Hayden, M. R. (1999) *Nat. Genet.* **22,** 336–345
21. Beaven, S. W., and Tontonoz, P. (2006) *Annu. Rev. Med.* **57,** 313–329
22. Wójcicka, G., Jamroz-Wisniewska, A., Horoszewicz, K., and Beltowski, J. (2007) *Postepy Hig. Med. Dosw.* **61,** 736–759
23. Jamroz-Wisniewska, A., Wójcicka, G., Horoszewicz, K., and Beltowski, J. (2007) *Postepy Hig. Med. Dosw.* **61,** 760–785
24. Zelcer, N., Khanlou, N., Clare, R., Jiang, Q., Reed-Geaghan, E. G., Landreth, G. E., Vinters, H. V., and Tontonoz, P. (2007) *Proc. Natl. Acad. Sci. U.S.A.* **104,** 10601–10606
25. Schultz, J. R., Tu, H., Luk, A., Repa, J. J., Medina, J. C., Li, L., Schwendner, S., Wang, S., Thoolen, M., Mangelsdorf, D. J., Lustig, K. D., and Shan, B. (2000) *Genes Dev.* **14,** 2831–2838
26. Lund, E. G., Peterson, L. B., Adams, A. D., Lam, M. H., Burton, C. A., Chin, J., Guo, Q., Huang, S., Latham, M., Lopez, J. C., Menke, J. G., Milot, D. P., Mitnaul, L. J., Rex-Rabe, S. E., Rosa, R. L., Tian, J. Y., Wright, S. D., and Sparrow, C. P. (2006) *Biochem. Pharmacol.* **71,** 453–463
27. Miao, B., Zondlo, S., Gibbs, S., Cromley, D., Hosagrahara, V. P., Kirchgess-

ner, T. G., Billheimer, J., and Mukherjee, R. (2004) *J. Lipid Res.* **45,** 1410–1417

28. Koldamova, R. P., Lefterov, I. M., Staufenbiel, M., Wolfe, D., Huang, S., Glorioso, J. C., Walter, M., Roth, M. G., and Lazo, J. S. (2005) *J. Biol. Chem.* **280,** 4079–4088

29. Riddell, D. R., Zhou, H., Comery, T. A., Kouranova, E., Lo, C. F., Warwick, H. K., Ring, R. H., Kirksey, Y., Aschmies, S., Xu, J., Kubek, K., Hirst, W. D., Gonzales, C., Chen, Y., Murphy, E., Leonard, S., Vasylyev, D., Oganesian, A., Martone, R. L., Pangalos, M. N., Reinhart, P. H., and Jacobsen, J. S. (2007) *Mol. Cell. Neurosci.* **34,** 621–628

30. Vanmierlo, T., Rutten, K., Dederen, J., Bloks, V. W., van Vart-van der Zee, L. C., Kuipers, F., Kiliaan, A., Blokland, A., Sijbrands, E. J. G., Steinbusch, H., Prickaerts, J., Lutjohann, D., and Mulder, M. (2009) *Neurobiol. Aging*

31. Groot, P. H., Pearce, N. J., Yates, J. W., Stocker, C., Sauermelch, C., Doe, C. P., Willette, R. N., Olzinski, A., Peters, T., d'Epagnier, D., Morasco, K. O., Krawiec, J. A., Webb, C. L., Aravindham, K., Jucker, B., Burgert, M., Ma, C., Marino, J. P., Collins, J. L., Macphee, C. H., Thompson, S. K., and Jaye, M. (2005) *J. Lipid Res.* **46,** 2182–2191

32. Jankowsky, J. L., Fadale, D. J., Anderson, J., Xu, G. M., Gonzales, V., Jenkins, N. A., Copeland, N. G., Lee, M. K., Younkin, L. H., Wagner, S. L., Younkin, S. G., and Borchelt, D. R. (2004) *Hum. Mol. Genet.* **13,** 159–170

33. Hamon, Y., Broccardo, C., Chambenoit, O., Luciani, M. F., Toti, F., Chaslin, S., Freyssinet, J. M., Devaux, P. F., McNeish, J., Marguet, D., and Chimini, G. (2000) *Nat. Cell Biol.* **2,** 399–406

34. Ennaceur, A., and Delacour, J. (1988) *Behav. Brain Res.* **31,** 47–59

35. Walf, A. A., Rhodes, M. E., and Frye, C. A. (2006) *Neurobiol. Learn Mem.* **86,** 35–46

36. Morris, R. (1984) *J. Neurosci. Methods* **11,** 47–60

37. DeMattos, R. B., Bales, K. R., Parsadanian, M., O'Dell, M. A., Foss, E. M., Paul, S. M., and Holtzman, D. M. (2002) *J. Neurochem.* **81,** 229–236

38. Chang, K. A., and Suh, Y. H. (2005) *J. Pharmacol. Sci.* **97,** 461–471

39. Glabe, C. G. (2008) *J. Biol. Chem.* **283,** 29639–29643

40. Bellgowan, P. S., Buffalo, E. A., Bodurka, J., and Martin, A. (2009) *Learn. Mem.* **16,** 433–438

41. Grimm, M. O., Grimm, H. S., Pätzold, A. J., Zinser, E. G., Halonen, R., Duering, M., Tschäpe, J. A., De Strooper, B., Müller, U., Shen, J., and Hartmann, T. (2005) *Nat. Cell Biol.* **7,** 1118–1123

42. Lefterov, I., Bookout, A., Wang, Z., Staufenbiel, M., Mangelsdorf, D., and Koldamova, R. (2007) *Mol. Neurodegener.* **2,** 20

43. Mahley, R. W., and Rall, S. C., Jr. (2000) *Annu. Rev. Genomics Hum. Genet* **1,** 507–537